

25 June 2018

# Resonant 3-photon ionization of hydrogenic atoms by non-monochromatic laser field

V Yakhontov<sup>†‡</sup>, R Santra<sup>§</sup> and K Jungmann<sup>§</sup>

<sup>†</sup> Mathematical Institute, University of Oxford, St. Giles' 24-29, Oxford OX1 3LB, UK, and at

<sup>§</sup> Physikalisches Institut der Universität Heidelberg, Philosophenweg 12, D-69120 Heidelberg, Germany

**Abstract.** We present ionization probability and line shape calculations for the two-step 3-photon ionization process,  $1S \xrightarrow{2\hbar\omega} 2S \xrightarrow{\hbar\omega} \varepsilon P$ , of the ground state of hydrogenic atoms in a non-monochromatic laser field with a time-dependent amplitude. Within the framework of a three-level model, the *AC Stark* shifts and non-zero ionization rates of all states involved were taken into account together with spatial and temporal inhomogeneities of the laser signal. In contrast with the usual perturbative technique, the time evolution of the atomic states was simulated by direct numerical solving the system of coupled time-dependent inhomogeneous differential equations, being equivalent to the appropriate non-stationary Schrödinger equation. Particular numerical results were obtained for typical parameters of the pulsed laser field that are employed in a new experiment to measure the  $1S - 2S$  energy separation in muonium at the Rutherford Appleton Laboratory. The shifts and asymmetries of the photoionization line shapes revealed may be of relevance for ultra-high precision experiments in hydrogen in CW laser fields.

PACS numbers: 32.60, 32.80, 36.10

Submitted to: *J. Phys. B: At. Mol. Opt. Phys.*

<sup>‡</sup> On leave from St.Petersburg State Technical University, Polytechnicheskaya 29, 195251, St. Petersburg, Russia. E-mail address: yakhon@maths.ox.ac.uk

## 1. Introduction

The dynamics of relaxing quantum systems in sufficiently strong laser fields, which are neither stationary nor monochromatic, is an important aspect of the theory of interaction between atoms and photon fields. This problem is of particular practical significance because of dramatic advances in the precision of measurements presently attainable in spectroscopic experimental studies of hydrogenic and few-particle atoms. Among the simple atoms that attracted attention in the last few years one should mention: *hydrogen* and its isotopes [1, 2, 3, 4, 5], *positronium* [6, 7], denoted  $(e^+ - e^-)$ , *muonium* (see [8, 9, 7, 10, 11] and references therein), denoted  $(\mu^+ - e^-)$ , and *helium* atom [12]. The measurements of the ground state HFS and the Lamb shift are of particular interest for these systems. High precision spectroscopy of low-lying transitions in hydrogenic atoms offers a unique opportunity to test QED calculations and to refine both the fundamental constants and various properties of respective nuclei. This urges further theoretical developments intended to describe the well established photon-induced processes in simple atoms with much higher precision than techniques used so far are able to provide, in order to allow a proper interpretation of newly available experimental data. In the present paper the stepwise 3-photon ionization of muonium in a *non-monochromatic* laser field with a *time-dependent* amplitude is studied.

It has been recognized already a long time ago (see [13] for a more detailed discussion) that the  $1S - 2S$  transition offers unique opportunities for high precision spectroscopy due to the narrow natural line width,  $\Gamma_{2s}^{(\text{nat})}$ , of the  $2S$ -state. In the hydrogen atom, for example,  $\Gamma_{2s}^{(\text{nat})} \approx 1.3$  Hz which enables the quality factor of  $\delta\nu/\nu \simeq 10^{-15}$  to be achieved already today, as well as suggests future resolutions of order of 1 part in  $10^{18}$ . Experimentally, the  $1S - 2S$  transition can be induced Doppler-free by absorbing two photons from two counter-propagating laser beams. In particular, this scheme is presently used at the Rutherford Appleton Laboratory [8] for determination of the  $1S - 2S$  energy separation in muonium to the 1 MHz accuracy. This study offers an opportunity to improve the present knowledge of the muon/electron mass ratio and, thereby, of the muon mass itself. In the course of this investigation, two counter-propagating pulsed laser beams with almost identical intensities,  $I(x, y, t)$ ,  $I_{\text{max}} \approx 10^6$  W/cm<sup>2</sup>, and the same photon energies,  $h\nu_L \approx 3/16$  a.u. ( $\lambda_L = 244$  nm) are used. Thus, the frequency  $\nu_L$  is such that it is tuned into resonance with the 2-photon Doppler-free  $1S \xrightarrow{2h\nu_L} 2S$  transition. Unlike the hydrogen case however, the  $1S - 2S$  transition in muonium is hard to be observed directly, i.e. by detecting radiation emitted as a result of the  $2S$ -state deexcitation. This is due to the fact that the appropriate line intensities in muonium happen to be weaker by several orders of magnitude, owing to much lower densities at which muonium atoms can be produced. Furthermore, the latter reason necessitates the use of higher laser intensities (by a factor of  $10^4$ , at least) that are required for a reasonable signal strength. This demands a *pulsed* rather than a CW laser source (as in the case of hydrogen [5]) to be employed. The  $2S$ -state of muonium is detected therefore via its photoionization by the third photon absorbed

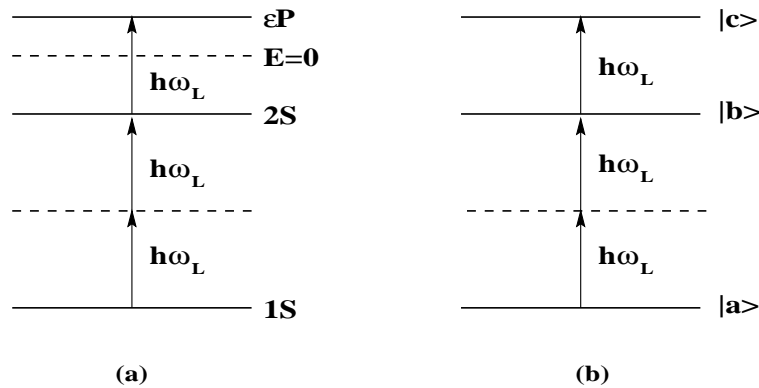


**Figure 1.** (a) – The scheme of the new 1S-2S experiment in muonium. (b) – The set of states to model the stepwise 3-photon ionization.

from one of the laser beams [8]. Schematically, the experiment in muonium is presented in figure 1(a) where  $\hbar\omega_L \approx 3/16$  a.u. ( $\nu_L \equiv \omega_L/2\pi \simeq 10^9$  MHz) stands for the resonant energy (frequency) which drives the 2-photon  $1S - 2S$  transition.

Despite the fact that the laser frequency can be calibrated, in principle, to a rather high accuracy, there are a number of systematic error sources each of which proves to be essential for precise determination of the  $1S - 2S$  energy separation in muonium. In this paper we report the results of the theoretical study intended to allow for one of the most important among these effects, that is, the time-dependent frequency variation (chirp) of the laser field. This phenomenon arises due to the rapid refraction index variation of the *laser media* and is hardly avoidable, especially with powerful pulsed lasers, unless some technical developments are made in order to compensate the frequency alteration [8, 12]. As will be demonstrated below, the chirped laser signal immediately makes its appearance in appreciable spurious shifting and broadening of spectral/photoionization lines, as well as leads to a noticeable distortion of the line shapes. To estimate the scale of the effect considered, one should note, for example, that the chirp-induced shift of the center of the ionization line is roughly equal to a characteristic magnitude of the chirp itself. For the  $1S - 2S$  experiment in muonium, the latter can typically amount to  $\delta/2\pi \simeq 10 \dots 100$  MHz, thus leading to the relative shift of the line's center by  $\delta/\omega_L \simeq 10^{-8} \dots 10^{-7}$ . The effects of such an order are usually completely neglected in atomic physics. Nonetheless, these happen to be crucial for studies where an absolute accuracy of 1 MHz is anticipated. It is therefore of primary practical importance to work out a relatively simple theoretical scheme which could allow one to describe certain types of multi-photon ionization phenomena in hydrogenic atoms, where an arbitrary time variation of the frequency of the laser field is accompanied by an arbitrary time modulation of its amplitude.

Although the problem of the hydrogenic systems' interaction with monochromatic resonant laser field with/without the amplitude modulation is investigated quite fully by now (see [14, 15, 16, 13, 17, 4] and references therein), there have been much fewer studies where both the amplitude and the frequency of the laser signal vary with time. Even

though, the authors confine themselves in most cases to either 1-photon (rather than 2-photon) resonant transition [18], or treat only somewhat special forms (“abrupt step”, “exponential field pulses” etc.) of the field modulation [19]. Under these circumstances, it seems very desirable to reconsider the problem as a whole, while adapting it specifically to the conditions of the  $1S - 2S$  experiment in muonium.

## 2. Theory

### 2.1. Basic equations

We consider, without a loss of generality, a set of three levels:  $|a\rangle$ ,  $|b\rangle$  and  $|c\rangle$ , of a hydrogenic atom with the charge  $Z$  of its nucleus, such that their one-particle energies satisfy the inequality:  $\varepsilon_a < \varepsilon_b < \varepsilon_c$ ; this rather general setup is shown in figure 1(b). It is supposed that the given 3-level system is exposed to two counter-propagating (along the  $z$ -axis) laser waves with equal time-dependent (circular) frequencies,  $\omega(t) \equiv \omega_L + \frac{1}{t}\phi(t)$ , polarizations vectors,  $\boldsymbol{\epsilon}$ , and wave vectors,  $\mathbf{k}_1(t) = -\mathbf{k}_2(t) \equiv \mathbf{k}(t)$ ,  $|\mathbf{k}(t)| = \alpha\omega(t)$ , where  $\alpha = e^2/(\hbar c) \approx 1/137$  is the fine structure constant and  $c$  denotes the speed of light. The stationary part,  $\omega_L$ , of the field frequency  $\omega(t)$  is assumed to be such that it is in the 2- and 1-photon resonances with the pairs of states,  $(|a\rangle, |b\rangle)$  and  $(|b\rangle, |c\rangle)$ , respectively. This implies that  $2\pi\nu_L \equiv \omega_L = \omega_{b,a}/2 = \omega_{c,b}$  with  $\omega_{j,i} \equiv \varepsilon_j - \varepsilon_i$ , ( $i, j = a, b, c$ ) being the differences of the one-particle energies. In addition, it is supposed that the  $E1$ -transition is forbidden between  $|a\rangle$  and  $|b\rangle$  and is allowed between  $|b\rangle$  and  $|c\rangle$ .

Under the resonance conditions assumed above, 3-photon ionization of the system, that is,  $|a\rangle \xrightarrow{3\hbar\omega_L} |c\rangle$  transition, occurs predominantly as a 2-step process: (i) a 2-photon resonant absorption from the state  $|a\rangle$  into the state  $|b\rangle$ , followed by (ii) a 1-photon resonant transition between the levels  $|b\rangle$  and  $|c\rangle$ . This simple physical picture is a consequence of the evident estimate of the probability for an atom to absorb 3 photons of equal energies (the atomic units,  $e = \hbar = m_e = 1$ , are used throughout the paper; in this system, the speed of light is equal to  $c \approx 137$ ):

$$W_{c,a}^{(3)}(\text{res}) \propto \frac{\Gamma_a}{\overline{\Delta\omega}^2} W_{b,a}^{(2)}(\text{res}) W_{c,b}^{(1)}(\text{res}). \quad (1)$$

Here,  $W_{b,a}^{(2)}(\text{res})$ ,  $W_{c,b}^{(1)}(\text{res})$  are the 2- and 1-photon resonant transition probabilities,  $\Gamma_a$  is the total width of the state  $|b\rangle$ , and  $\overline{\Delta\omega}$  denotes some characteristic mean energy which a two-fold summation over intermediate states in the exact expression to define  $W_{c,a}^{(3)}(\text{res})$  (see [20] for a more detailed discussion) can be reduced to. Equation (1) readily follows then from the estimate,  $\Gamma_a/\overline{\Delta\omega}^2 \ll 1$ , which is fulfilled for most states of atoms in moderately strong laser fields, except extraordinarily short-living ones. A situation when  $|a\rangle$  stands for the ground-,  $|b\rangle$  for the  $2S$ -, and  $|c\rangle$  for the continuum  $\varepsilon P$ -states, respectively, is of our primary concern here. In this case  $\overline{\Delta\omega}^2 \simeq 1$  and  $\Gamma_{2s}^{(\text{tot})}/\overline{\Delta\omega}^2 \simeq 10^{-9}$  since  $\Gamma_{2s}^{(\text{tot})} = \Gamma_{2s}^{(\text{nat})} + \Gamma_{2s}^{(\text{phot})} \simeq 10^{-9}$  is dominated by the photoionization rate of the  $2S$ -level ( $\Gamma_{2s}^{(\text{phot})} \simeq 10^{-9} \gg \Gamma_{2s}^{(\text{nat})} \simeq 10^{-15}$ ). Accordingly, we will assume that the natural line widths of the  $|a\rangle$ - and  $|b\rangle$ -levels are both equal to zero:  $\Gamma_a^{(\text{nat})} = \Gamma_b^{(\text{nat})} = 0$ . A

straightforward generalization of the latter condition, that might be required for the treatment of *excited* states, can be achieved by adding appropriate imaginary parts to the energies of the levels [21]:  $\varepsilon_a \rightarrow \varepsilon_a - i\Gamma_a^{(\text{nat})}/2$ ,  $\varepsilon_b \rightarrow \varepsilon_b - i\Gamma_b^{(\text{nat})}/2$ .

In the semiclassical approximation, which happens to be accurate enough for our purposes, the electric fields inducing the 2- and 1-photon transitions can be taken in the form

$$\mathbf{E}_{1,2}(\mathbf{r}, t) = \frac{1}{2}\boldsymbol{\varepsilon}E_{1,2}(t)U_{1,2}(\mathbf{r}) \exp\{i(\mathbf{k}_{1,2}(t)\mathbf{r} - \omega(t)t)\} + c.c. \quad (2)$$

Here, the real functions  $U_1(\mathbf{r}) = U_2(\mathbf{r}) \equiv U(\mathbf{r})$  and  $E_1(t) = E_2(t) \equiv E(t)$  describe the (macroscopic) spatial inhomogeneity of the laser field and its time-dependent amplitude. These are related direct to the laser intensity  $I(\mathbf{r}, t)$  which, along with the chirped (circular) laser frequency  $\omega(t)$ , is obtainable direct from measurements. For the 1S–2S experiment with muonium,  $I(\mathbf{r}, t)$  and  $\omega(t)$  can be well approximated as [22]:

$$I(\mathbf{r}, t) \equiv \frac{c}{8\pi}E^2(t)U^2(\mathbf{r}) = \frac{1}{(2\pi)^{3/2}}\frac{A_\omega}{\sigma_t\sigma_r^2} \exp\left\{-\frac{t^2}{2\sigma_t^2} - \frac{x^2 + y^2}{2\sigma_r^2}\right\}, \quad (3)$$

$$\omega(t) \equiv \omega_L + \frac{1}{t}\phi(t) \approx \omega_L + \dot{\phi}(t) \equiv \omega_L + \frac{1}{2}\delta(1 + \text{erf}(t/\tau)), \quad (4)$$

where  $A_\omega = 2\dots 5$  mJ is the energy within one laser pulse;  $\sigma_t = 40\dots 65$  ns,  $\sigma_r = 0.5\dots 1.5$  mm denote the temporal and spatial dispersions of the external laser field (in the  $XOY$  plane perpendicular to the direction of the beams' propagation). The full temporal width of the laser pulse is expressed then as  $\tau = 2\sqrt{2\ln 2} \cdot \sigma_t = 100\dots 150$  ns. Parameter  $\delta \equiv \omega_L(+\infty) - \omega_L(-\infty) \simeq 2\pi \cdot (10\dots 100)$  MHz defines the magnitude of the chirp  $\dot{\phi}(t)$ , being actually detected in the experiment, and  $\text{erf}(\dots)$  stands for the error function [23].

As usually happens to be true in most practical situations, both the amplitude  $E(t)$  and the additional phase  $\phi(t)$  vary much slower with time than  $\mathbf{E}(t)$  and  $\omega(t)$  (see equations (3)-(4)). In addition, the magnitude of the chirp is normally much smaller than the ‘‘base’’ frequency  $\omega_L$ . It is therefore permissible to assume that  $\omega(t)$  and  $E(t)$  are subject to the following general conditions [24, 25]:

$$|t\dot{\omega}(t)| \ll |\omega(t) - \omega_L| \equiv \left|\frac{1}{t}\phi(t)\right| \approx |\dot{\phi}(t)| \ll \omega_L \quad (5)$$

$$\left|\dot{E}(t)\right| \ll |\omega_L E(t)|. \quad (6)$$

Within the framework of the conventional time-dependent perturbation theory [21], the exact time-dependent wave function of the quasi-stationary state  $\psi_n(t)$  in the field is sought in the form

$$\psi_n(t) = \sum_k c_{k,n}(t)\psi_k^{(0)}e^{-i\varepsilon_k t}, \quad (7)$$

where  $c_{k,n}(t)$ , being the amplitudes to find an atom in one of the unperturbed states  $\psi_k^{(0)}$ , satisfy the following well known system of coupled differential equations:

$$\dot{c}_{k,n}(t) = -i \sum_s V_{k,s}(t)c_{s,n}(t)e^{-i\omega_{k,s}t}. \quad (8)$$

Here,  $V_{k,s}(t)$  denotes the matrix element of  $V(t)$  being the operator of the “particle–laser field” interaction. Due to the given below reasons,  $V(t)$  can be taken in the form

$$V(t) \approx -\mathbf{E}(\mathbf{r}, t) \cdot \mathbf{d} \approx -\frac{1}{2}E(t)U(\mathbf{r})e^{-i\omega(t)t}\boldsymbol{\epsilon} \cdot \mathbf{d} + c.c. \quad (9)$$

where  $\mathbf{d}$  is the dipole operator of an electron (or a muon) and  $\mathbf{E}(\mathbf{r}, t)$  denotes the electric field (2) seen by the atom in its rest frame. For particular laser parameters of interest, the accuracy of the above approximation follows from the evident estimate:  $|\nabla U(\mathbf{r})| \simeq 1/\sigma_r \approx 10^{-7} \ll |\mathbf{k}(t) \cdot \mathbf{r}| \simeq 2\pi/\lambda_L \approx 10^{-3}$ . This implies that the contribution of the quadrupole terms  $\propto E(t)(\nabla U(\mathbf{r}) \cdot \mathbf{d})$ , which originate from the spatial *macroscopic* inhomogeneity of  $\mathbf{E}(\mathbf{r}, t)$ , is expected to be a factor  $10^{-7}$  smaller than the contribution of the (dipole) terms in (9). Almost the same estimate holds also for corrections arising due to the quadrupole component  $\propto E(t)U(\mathbf{r})|\mathbf{k}(t)|(\boldsymbol{\epsilon} \cdot \mathbf{d})^2$  of the photon field itself. This is despite the fact that the states  $|a\rangle$  and  $|b\rangle$  are coupled, in accord with the initial assumptions of our model and equation (9), in only the second order of the perturbation theory in  $V(t)$ , i.e. by taking into account at least the 2-photon absorption/emission. Indeed, unlike the second order dipole coupling, the 1-photon quadrupole  $|a\rangle \leftrightarrow |b\rangle$  transition would apparently be off resonance. This would makes its appearance in the extra exponential factor  $\simeq e^{i\omega_L t}$  in the amplitude. If  $V_{a,b} \ll \omega_L$ , as it is assumed throughout the paper, then the terms of such a type are known to be almost negligible [26]. In our case, in particular, their relative contribution is of the order of  $1/(\omega_L \tau) \simeq 10^{-8}$ , as can be shown by averaging the transition amplitude over some time interval:  $-T < t < T \simeq \tau$ . The same “off-resonant” argument is fully applicable to magnetic transitions as well, thus elucidating why the  $M1$ - and  $E2$ -contributions are suppressed by a factor  $\simeq 10^{-8}$  as compared to the dipole one.

By virtue of (8)-(9), one can readily retrieve, after some conventional algebra, the following form for effective quasiclassical one-particle operators which couple two given states of reference [17, 13]:

$$V_{b \leftarrow a}^{(\text{eff})}(\mathbf{r}, t, \omega_L) = \frac{1}{4}U^2(\mathbf{r})E^2(t)e^{-2i(\omega_L t + \phi(t))} \sum_s \frac{\langle b | \mathbf{d} \cdot \boldsymbol{\epsilon} | s \rangle \langle s | \mathbf{d} \cdot \boldsymbol{\epsilon} | a \rangle}{\omega_{a,s} + \omega_L}, \quad (10)$$

$$V_{b \rightarrow a}^{(\text{eff})}(\mathbf{r}, t, \omega_L) = \frac{1}{4}U^2(\mathbf{r})E^2(t)e^{2i(\omega_L t + \phi(t))} \sum_s \frac{\langle a | \mathbf{d} \cdot \boldsymbol{\epsilon}^* | s \rangle \langle s | \mathbf{d} \cdot \boldsymbol{\epsilon}^* | b \rangle}{\omega_{b,s} - \omega_L}, \quad (11)$$

$$V_{b,b}^{(\text{eff})}(\mathbf{r}, t, \omega_L) = \frac{1}{4}U^2(\mathbf{r})E^2(t) \sum_s \left\{ \frac{|\langle b | \mathbf{d} \cdot \boldsymbol{\epsilon} | s \rangle|^2}{\omega_{b,s} + \omega_L} + \frac{|\langle b | \mathbf{d} \cdot \boldsymbol{\epsilon} | s \rangle|^2}{\omega_{b,s} - \omega_L} \right\}. \quad (12)$$

All summations are performed here over complete set of one-particle atomic orbitals. Equations (10)-(11) describe the real transitions, whereas (12) defines the *AC Stark* shift of the level  $|b\rangle$  (or  $|a\rangle$ , if  $b \rightarrow a$ ) which arises due to interaction of the atom with the incident radiation. Note that the sum in (12) coincides, by definition [21], with the dipole dynamic polarizability of the state  $|b\rangle$  at the frequency  $\omega$ . Also, it should be pointed out that only the leading terms, as given by equations (10)-(12), were retained

in the course of derivation. The most important among neglected terms are of the form:

$$U^2(\mathbf{r}) \left| \frac{i}{\omega_{s,a} - \omega_L} \left( \frac{\dot{E}(t) - iE(t)\dot{\phi}(t)}{\omega_{s,a} - \omega_L} e^{i[(\omega_{s,a} - \omega_L)t - \phi(t)]} + c.c. \right) \right|^2 \simeq \frac{1}{\omega_L^4} |\dot{E}(t)|^2 U^2(\mathbf{r}).$$

Apparently, this contribution is smaller than  $V_{i \leftrightarrow j}^{(\text{eff})}(\mathbf{r}, t, \omega_L)$ , ( $i, j = a, b$ ) by a factor of  $|\dot{E}(t)/(\omega_L E(t))|^2 \simeq 1/(\omega_L \tau) \simeq 10^{-8}$ , as follows from (3)-(4), in accord with (5)-(6).

As was assumed above, there are no other discrete resonant atomic levels (either 1- or 2-photon) except  $|a\rangle$ ,  $|b\rangle$ . This enables the system (8) to be reduced to these two states only §, while describing the 1st stage of the two-step 3-photon ionization process under consideration. Indeed, an inclusion of the off-resonant states would give rise in the right-hand side of equations (14)-(15) to the rapidly  $t$ -varying terms  $\simeq e^{\pm i\omega_L t}$ . After temporal averaging (see above), these happen to be of order of  $1/(\omega_L \tau) \simeq 10^{-8}$ , and can therefore be omitted to the accuracy adopted in this study. On introducing the new functions,

$$c_{a,a}(t) \equiv e^{-i\alpha(t)}, \quad C(t) \equiv c_{b,a}(t) \exp \left\{ i \left[ 2 \left( \omega - \frac{1}{2} \omega_{b,a} \right) + \alpha(t) + 2\phi(t) \right] \right\}, \quad (13)$$

and replacing the matrix elements in (8) by equations (10)-(12), one arrives at the following system of equations:

$$\dot{\alpha}(t) = \frac{4\pi}{c} I(\mathbf{r}, t) [D_{a,a} + D_{a,b} C(t)], \quad (14)$$

$$\dot{C}(t) = -i D_{b,a} \frac{4\pi}{c} I(\mathbf{r}, t) - i \left[ D_{b,b} \frac{4\pi}{c} I(\mathbf{r}, t) - \left( 4\pi \Delta\nu + \dot{\alpha}(t) + 2\dot{\phi}(t) \right) \right] C(t), \quad (15)$$

where  $2\pi \Delta\nu \equiv \omega_L - \omega_{b,a}/2$  is the time-independent frequency detuning off the resonance,  $I(\mathbf{r}, t) = cE^2(t)U^2(\mathbf{r})/8\pi$  is the intensity of the single laser beam and  $D_{j,i}$ , ( $j, i = a, b$ ) denote the effective matrix elements given by the sums in (10)-(12). It has been taken into account here that the 3-level system is actually probed by a superposition of two laser fields (2), rather than by a single one; this results eventually in doubling all matrix elements. In addition, we have neglected a contribution due to the 2-photon absorption from *each* of two laser beams. This contribution comes from the second-order interactions of an atom with only one of two light waves and makes its appearance finally in two Doppler-broadened terms, i.e. depending on a  $v_z$ -component of atomic velocity in the laboratory frame, in the expression to define ionization probabilities. However, after averaging over  $v_z$ , as would be required within the framework of a systematic approach, these terms turn out to be small compared, at the center of the photoionization line [27, 28], with the Doppler-free ones which originate from (14)-(15). These arguments provide the ground for the approximation made, although the effects caused by atomic movement in the media are beyond the scope of our present consideration.

It is relevant to point out here that the matrix elements,  $D_{j,i}$ , ( $j, i = a, b$ ) in (14)-(15) are  $\omega_L$ -dependent. In particular,  $D_{b,b}$  has a non-zero imaginary part. The latter

§ This implies that the Coulomb degeneracy of the levels with the same principal quantum number, say  $|ns\rangle$  and  $|nd\rangle$ , is ignored, since we are mainly concerned here with the lowest  $1S$ - and  $2S$ -states.

allows for a non-zero photoionization rate of the  $|b\rangle$ -state, due to the action of the photon field, since  $\omega_L$  is supposed to exceed the photoionization threshold  $I_b$ . Indeed, as was noted above,  $D_{b,b}$  is proportional to the dynamic (tensor) polarizability  $\alpha_b^{ij}(\omega_L)$  of the level  $|b\rangle$ , which is complex-valued if  $\omega_L \geq I_b$  (see our recent paper [31] for a more detailed discussion).  $\Re\alpha_a^{ij}(\omega)$  and  $\Im\alpha_a^{ij}(\omega)$  define then the *AC Stark* shift of the level (see equation (12)) and its decay probability ( $\propto |V_{bc}|^2$ ) via the single photoionization. This result is in agreement with the optical theorem [20]:  $\sigma_b^{(\gamma)}(\omega_L) = 4\pi\alpha\omega_L\Im\alpha_b^{ij}(\omega_L)$ , where  $\alpha$  is the fine structure constant and  $\sigma_b^{(\gamma)}(\omega_L)$  denotes the total photoionization cross section of the state  $|b\rangle$ . Numerical calculations show that the single photoionization happens to be the main channel of the  $|b\rangle$ -level depopulation. It is therefore crucial for the correct description of the time-evolution of the 3-level system that this depopulation mechanism is taken in fact into account in (14)-(15) through the matrix elements  $D_{j,i}$ ,  $(j, i) = a, b$ .

An allowance for the 2nd step of the process considered can be made by augmenting the system (14)-(15) with an additional equation that explicitly describes the  $|b\rangle - |c\rangle$  coupling through the single photoionization of the state  $|b\rangle$ . Given by (16c), this extra equation is nothing else but a differential form of the conservation law which determines the probability balance between the states of reference. Moreover, equations (14)-(15) can be decoupled by substituting  $\dot{\alpha}(t)$  of (14) into (15) to finally get

$$\dot{C}(t) = -iD_{b,a}\frac{4\pi}{c}I(\mathbf{r}, t) + i\left[(D_{a,a} - D_{b,b})\frac{4\pi}{c}I(\mathbf{r}, t) + 2\left(2\pi\Delta\nu + \dot{\phi}(t)\right)\right]C(t) \quad (16a)$$

$$+ iD_{b,a}\frac{4\pi}{c}I(\mathbf{r}, t)C^2(t),$$

$$\dot{\alpha}(t) = \frac{4\pi}{c}I(\mathbf{r}, t)[D_{a,a} + D_{b,a}C(t)], \quad (16b)$$

$$\dot{W}_c(t) = \frac{2}{\omega_L}\sigma_b^{(\gamma)}(\omega_L)I(\mathbf{r}, t)|C(t)|^2 \exp\{2\Im\alpha(t)\}, \quad (16c)$$

where  $W_c(t)$  is the probability for an atom to be ionized by the time  $t$ , via absorption of 3 photons of equal energy. Under the actual experimental conditions [8], initial population of the level  $|b\rangle$ , i.e. before the laser pulse is shot, is usually rather low. This is because the major fraction of the muonium atoms is produced in the *ground* state  $|a\rangle$  where the population is proportional to  $|c_{a,a}|^2 \equiv \exp\{2\Re\alpha(t)\}$ . In view of this physical picture and by virtue of (13), it is natural to impose the following initial conditions on the functions  $\alpha(t)$ ,  $C(t)$ ,  $W_c(t)$ :

$$C(-\infty) = 0, \quad \alpha(-\infty) = 0, \quad W_c(-\infty) = 0. \quad (17)$$

These enable  $W_c(t = +\infty, \Delta\nu, A_\omega, r; [\phi])$  to be determined uniquely. Being of our primary concern, this quantity constitutes the required 3-photon resonant ionization probability of an atom at infinitely large positive times, i.e. when the interaction between the single laser pulse and the system has already ceased. As a function of the laser frequency detuning  $\Delta\nu$ ,  $W_c(t = +\infty, \Delta\nu, A_\omega, r; [\phi])$  describes, and will be therefore used as a synonym of, the 3-photon ionization line profile/shape. For brevity, the latter will be denoted as  $W_c^\infty(\Delta\nu, \delta, A_\omega, r; [\phi])$  where the argument  $[\phi]$  is introduced in order to indicate explicitly that the line profile depends on the form of the chirp.

In particular, if  $\dot{\phi}(t) \equiv \delta(1 + \text{erf}(t/\tau))/2$  then  $W_c^\infty(\Delta\nu, A_\omega, r; [\phi])$  will be denoted as simply  $W_c^\infty(\Delta\nu, A_\omega, \delta, r)$ .

Equations (16a)-(16c) are well suited for numerical calculations with arbitrary functions defining the spatial and temporal distributions of the laser pulse. In addition, the given system is rather convenient for analytic treatment, as will be demonstrated in subsection 2.2. In particular, one can develop further perturbative expansion of equations (16a)-(16b) in terms of the intensity  $I(\mathbf{r}, t)$ . This yields analytic formulae which, after setting  $\dot{\phi}(t) = 0$ , agree with those formerly derived in [17] within the framework of a 2-level model, for *unchirped* laser signals. Despite a relatively simple form of the appropriate equations, however, a not very straightforward numerical integration is still required in order to calculate, for example, photoionization line profiles in most practical situations, let alone the fact that the result of the work [17] is valid for rather weak laser intensities only. Note that equations (16a)-(16c) are free from the latter restriction. Furthermore, unlike our approach employing the probability amplitudes, the problems similar to those considered in this paper are usually treated (e.g. see [17, 12]) in the formalism of the density matrix [29]. Under the physical conditions adopted here, these two approaches are equivalent. To facilitate the adequate comparison however, it is relevant to present here an alternative form of (16a)-(16c), by rewriting the system in terms of the density matrix elements:  $\rho_{a,a}(t) \equiv |c_{a,a}(t)|^2$ ,  $\rho_{b,b}(t) \equiv |c_{b,a}(t)|^2$  and  $\rho_{b,a}(t) \equiv c_{b,a}(t)c_{a,a}^*(t) \exp\{-i 2(2\pi\Delta\nu t + \phi(t))\}$ , denoted as  $\rho_{b,a}(t) \equiv \gamma(t) + i\beta(t)$ . This yields:

$$\dot{\rho}_{b,b}(t) = \frac{8\pi}{c} \Im D_{b,b} I(\mathbf{r}, t) \rho_{b,b}(t) - \frac{8\pi}{c} D_{b,a} I(\mathbf{r}, t) \beta(t) \quad (18a)$$

$$\begin{aligned} \dot{\beta}(t) = & 2 \left( 2\pi\Delta\nu + \dot{\phi}(t) \right) \gamma(t) + \frac{4\pi}{c} I(\mathbf{r}, t) \{ (\Re D_{a,a} - \Re D_{b,b}) \gamma(t) \\ & + (\Im D_{a,a} + \Im D_{b,b}) \beta(t) \} + \frac{4\pi}{c} D_{b,a} I(\mathbf{r}, t) (\rho_{b,b}(t) - \rho_{a,a}(t)) \end{aligned} \quad (18b)$$

$$\dot{\rho}_{a,a}(t) = \frac{8\pi}{c} \Im D_{a,a} I(\mathbf{r}, t) \rho_{a,a}(t) + \frac{8\pi}{c} D_{b,a} I(\mathbf{r}, t) \beta(t) \quad (18c)$$

$$\begin{aligned} \dot{\gamma}(t) = & -2 \left( 2\pi\Delta\nu + \dot{\phi}(t) \right) \beta(t) + \frac{4\pi}{c} I(\mathbf{r}, t) \{ (\Re D_{b,b} - \Re D_{a,a}) \beta(t) \\ & + (\Im D_{a,a} + \Im D_{b,b}) \gamma(t) \} \end{aligned} \quad (18d)$$

$$\dot{W}_c(t) = \frac{2}{\omega_L} \sigma_b^{(\gamma)}(\omega_L) I(\mathbf{r}, t) \rho_{b,b}(t). \quad (18e)$$

Here, 5 unknown functions are subject to the following initial conditions:

$$\rho_{a,a}(-\infty) = 1, \quad \rho_{b,b}(-\infty) = \gamma(-\infty) = \beta(-\infty) = W_c(-\infty) = 0. \quad (19)$$

It should be pointed out that only real quantities enter equations (18a)-(18e). This circumstance may be advantageous, especially for numerical calculations, since most standard numerical packages are not applicable direct to systems of ODE involving complex-valued coefficients. Apart from that, (16a)-(16c) and (18a)-(18e) generate identical results, as has been proved by extensive numerical tests carried out by us for laser signals with various forms of the chirp, pulse envelope, and spatial distribution.

However, before we demonstrate appropriate results (see section 3), it is instructive to present here an approximate but reasonably accurate analytic solution for  $C(x)$ . This consideration seems to be rather useful for a qualitative description of the process as a whole, since it reveals some key features which make their appearance due to the non-stationarity of both the frequency and the amplitude of the laser signal.

## 2.2. Some analytic consideration: equation (16a)

Let us assume, in agreement with (3), that the intensity of the incident radiation is Gaussian both in time and space and use the most general form of the chirp,  $\dot{\phi}(t/\tau)$  (cf. equation (4)).

To start with, consider Riccati-type equation (16a) to determine the complex-valued function  $C(x) : |C(x)| \equiv |c_{b,a}(t)|/|c_{a,a}(t)|$ , defined by (13). On introducing the dimensionless variable  $x \equiv t/\tau$ , equation (16a) takes the form

$$C''(x) - iD_{b,a}\mathcal{I}e^{-\frac{\tau^2 x^2}{2\sigma_t^2}} C^2(x) - i \left[ 4\pi\Delta\nu\tau + 2\dot{\phi}(x) + \mathcal{I}\Delta D e^{-\frac{\tau^2 x^2}{2\sigma_t^2}} \right] C(x) + iD_{b,a}\mathcal{I}e^{-\frac{\tau^2 x^2}{2\sigma_t^2}} = 0, \quad (20)$$

where the following notations were introduced for brevity:

$$\frac{4\pi}{c}\tau I(\mathbf{r}, t) \equiv \mathcal{I} \exp \left\{ -\frac{\tau^2 x^2}{2\sigma_t^2} \right\}, \quad \mathcal{I} \equiv \sqrt{\frac{2}{\pi c^2}} \frac{\tau A_\omega}{\sigma_t \sigma_r^2} \exp \left\{ -\frac{r^2}{2\sigma_r^2} \right\}, \quad (21)$$

$$\Delta D \equiv D_{a,a} - D_{b,b}.$$

Note that

$$\mathcal{I} = \sqrt{2\pi} \frac{2\tau}{c\sigma_t} \int_{-\infty}^{+\infty} I(\mathbf{r}, t) dt = 8.805 \cdot 10^{-3} \frac{(A_\omega/1 \text{ mJ})}{(\sigma_r/1 \text{ mm})^2} \exp \left\{ -\frac{r^2}{2\sigma_r^2} \right\} a.u.$$

depends on the time-independent parameters of the pulse only, but not on  $x$ .

Due to its non-linearity, equation (20) admits only numerically solving, except for the trivial case,  $\Delta\nu = \dot{\phi}(x) = 0$ , where  $C(x)$  is of the form

$$C(x) = \frac{1}{2D_{b,a}} \left\{ \sqrt{4D_{b,a}^2 + \Delta D^2} \tanh \left[ -i \frac{\sqrt{2\pi} \mathcal{I} \sigma_t}{4\tau} \sqrt{4D_{b,a}^2 + \Delta D^2} \left( 1 + \operatorname{erf} \left( \frac{\tau x}{\sqrt{2}\sigma_t} \right) \right) + \tanh^{-1} \left( \frac{\Delta D}{\sqrt{4D_{b,a}^2 + \Delta D^2}} \right) \right] - \Delta D \right\}. \quad (22)$$

However, the problem can be simplified considerably by linearizing equation (20). This approximation, which the consideration developed below is stemmed on, is justifiable if  $|C(x)|^2 \ll |C(x)| \ll 1$  holds uniformly for  $-\infty < x < +\infty$  and arbitrary  $\Delta\nu$ ,  $\delta$  and  $r$ . To satisfy the latter condition, it is sufficient (but not necessary) to assume that

$$\lambda \equiv |\mathcal{I}D_{b,a}(\omega_L)| \lesssim 1, \quad (23)$$

as readily follows from equation (25). If  $|a\rangle = 1s$ ,  $|b\rangle = 2s$  and  $r = 0$ , for example, then  $\lambda \simeq A_\omega |D_{2s,1s}(\omega_L)|/\sigma_r^2 \lesssim 1$ . This imposes the following restriction on the pulse

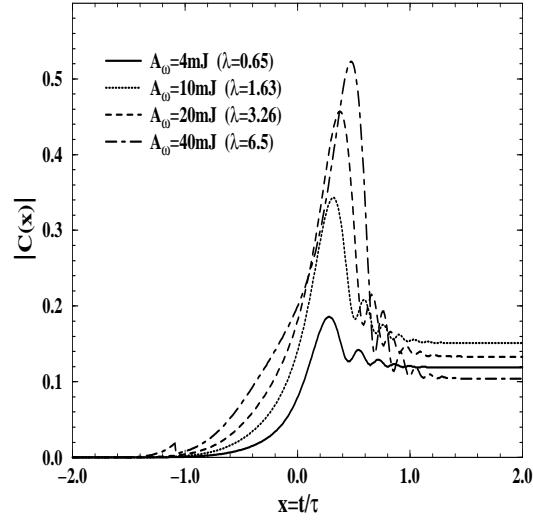


**Figure 2.**  $|C(x, \Delta\nu, \delta, A_\omega)|$  as a function of  $x$ , for various pulse energies,  $A_\omega$ , and fixed values of the chirp,  $\delta = 500 \text{ Mrad} \cdot \text{s}^{-1}$ , and the frequency detuning,  $\Delta\nu = -\delta/(4\pi) = -250/(2\pi) \text{ MHz}$ . The laser field frequency is assumed to be of the form:  $\nu(t) \equiv \nu_L + \nu_{\text{chirp}}(t) \equiv \nu_L + \frac{\delta}{4\pi} (1 + \text{erf}(t/\tau))$ ; the rest laser parameters used are:  $\sigma_t = 51 \text{ ns}$ ,  $\tau = 120 \text{ ns}$ ,  $r = 0$ .

energy:  $A_\omega \lesssim 6 \text{ mJ}$ , where particular values of the atomic matrix element,  $D_{2s,1s}(\omega_L)$  (see table 1), and the typical laser parameters have been used. The above estimates are illustrated in figure 2 where  $|C(x, \Delta\nu = -\delta/4\pi, \delta, A_\omega)|$  obtained by direct numerically solving equation (20) is plotted versus the dimensionless variable  $x$ , at several  $A_\omega$ -values. In addition, for each pulse energy, the appropriate  $\lambda$ -value defined by equation (23) is indicated for reference as well.

The linearized form of equation (20) reads:

$$\tilde{C}'(x) - i \left[ 4\pi\Delta\nu\tau + 2\dot{\phi}(x) + \mathcal{I}\Delta D e^{-\frac{\tau^2 x^2}{2\sigma_t^2}} \right] \tilde{C}(x) + iD_{b,a} \mathcal{I} e^{-\frac{\tau^2 x^2}{2\sigma_t^2}} = 0. \quad (24)$$

Its solution obeying the zero initial condition (17) at  $x = -\infty$  has the form

$$\begin{aligned} \tilde{C}(x) = & -iD_{b,a} \mathcal{I} \exp \left\{ ix (4\pi\tau\Delta\nu + 2\phi(x)/x) + i\sqrt{\frac{\pi}{2}} \frac{\sigma_t}{\tau} \mathcal{I}\Delta D \text{erf} \left( \frac{\tau x}{\sqrt{2}\sigma_t} \right) \right\} \\ & \times \int_{-\infty}^x \exp \left\{ -iu (4\pi\tau\Delta\nu + 2\phi(u)/u) - i\sqrt{\frac{\pi}{2}} \frac{\sigma_t}{\tau} \mathcal{I}\Delta D \text{erf} \left( \frac{\tau u}{\sqrt{2}\sigma_t} \right) - \frac{\tau^2 u^2}{2\sigma_t^2} \right\} du. \end{aligned} \quad (25)$$

To demonstrate the fair accuracy of this relation for  $A_\omega = 4 \text{ mJ}$  and  $\phi(x) = \delta\tau x (1 + \text{erf}(x))/2$ , for example, the graph of  $|\tilde{C}(x, \Delta\nu, \delta, A_\omega)| \simeq |c_{2s,1s}(t)|/|c_{1s,1s}(t)|$  as a function of  $x$  is presented, for several chirp values, in figure 3, along with appropriate graphs for numerical solution of the non-linear equation (20). Together with plots in figure 2, these graphs provide instructive information about the magnitude of  $|c_{2s,1s}(t)|^2/|c_{1s,1s}(t)|^2$  at various time moments. In addition, both figures clearly

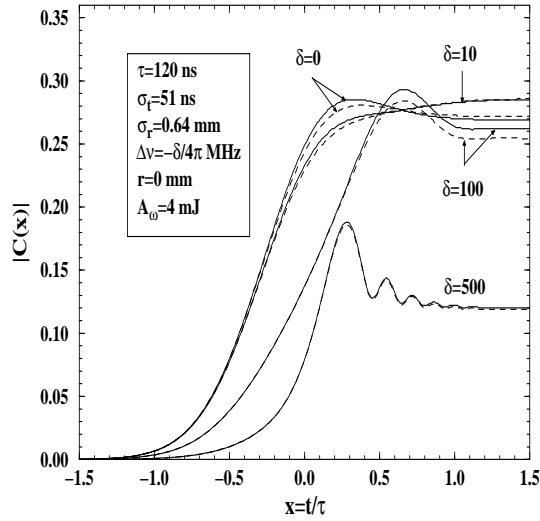


**Figure 3.**  $|C(x, \Delta\nu, \delta, A_\omega)|$  and  $|\tilde{C}(x, \Delta\nu, \delta, A_\omega)|$  as functions of  $x$ , for fixed values of the pulse energy,  $A_\omega = 4$  mJ, frequency detuning,  $\Delta\nu = -\delta/(4\pi)$  MHz, and for several chirp values:  $\delta = 0, 10, 100, 500$  Mrad  $\cdot$  s $^{-1}$ . The frequency of the non-monochromatic laser field is assumed to be of the form:  $\nu(t) \equiv \nu_L + \nu_{\text{chirp}}(t) \equiv \nu_L + \frac{\delta}{4\pi} (1 + \text{erf}(t/\tau))$ , and the rest laser parameters used are:  $\sigma_t = 51$  ns,  $\tau = 120$  ns,  $r = 0$ .  
— — numerical solution of equation (20); - - - - analytic solution,  $|\tilde{C}(x)|$ , of equation (24), as given by (25).

demonstrate a rather peculiar way in which the values for the above ratio are (strongly) distorted due the presence of the chirp.

It is relevant to note that  $\tilde{C}(x)$  approximates the function  $C(x)$  qualitatively correctly for even those  $A_\omega$  which violate condition (23). An elaborate comparison with exact numerical solutions of (20) shows that, for most applications, the region of the validity of equation (25) can be safely extended up to  $A_\omega \lesssim 20$  mJ, depending on the rest laser parameters. At higher pulse energies, the contribution of non-linear effects becomes so essential that the neglect of the  $\simeq C^2(x)$ -term is no longer permissible. This can be seen, for example, in figure 2 where, for  $|x| \lesssim 1$  and  $A_\omega = 20$  mJ, appropriate non-linear contribution amounts to 20%.

As follows from the method of our derivation, equation (25) can be readily generalized on a wide class of similar multi-photon ionization processes that are induced by not very intense laser fields and which involve the chirps and laser amplitudes, such that  $|\dot{\phi}(t)| \ll \omega_L$  and  $I(\mathbf{r}, t) \rightarrow 0$  sufficiently fast as  $t \rightarrow \pm\infty$ . Note that the latter condition ensures the rapid convergence of the integral in (25). In addition, it makes certain that the values of all physical quantities of interest are determined actually by only a somewhat narrow domain of  $x$  within which the laser intensity is peaked.

Equation (25) is suitable to be used further for the analytical study of the 3-photon ionization with muonium, where  $|a\rangle = 1s$ ,  $|b\rangle = 2s$  and  $\phi(x) \equiv \delta\tau x (1 + \text{erf}(x)) / 2$ . In particular,  $\tilde{C}(x)$  readily enables one to obtain analytic formulae for the probabilities:

$|c_{1s,1s}(t)|^2$ ,  $|c_{2s,1s}(t)|^2$ , and  $W_c^\infty(\Delta\nu, A_\omega, r; [\phi])$ . However, these expressions are not given explicitly here as they turn out to be too bulky. Instead, the formula (25) will be used in the following subsection 2.3, while addressing an interesting complementary problem: a calculation of the integral of the 3-photon ionization line profile over the entire range of the frequency detunings,  $-\infty < \Delta\nu < +\infty$ .

### 2.3. Further analytic consideration: the integral over the frequency detunings

In what follows, it is shown that, for given  $A_\omega$  and  $r$ , the integral of the 3-photon ionization line profile,  $W_c^\infty(\Delta\nu, A_\omega, r; [\phi])$ , over the entire range of the frequency detunings  $\Delta\nu$ ,

$$\rho(A_\omega, r; [\phi]) \equiv \int_{-\infty}^{+\infty} W_c^\infty(\Delta\nu, A_\omega, r; [\phi]) d\Delta\nu, \quad (26)$$

is almost independent of particular form of the chirp, at least for low pulse energies. To be more precise, equation (26) defines in fact a non-linear functional of  $\phi(t)$  whose “strength” depends, though, on the rest laser parameters. Within certain range of these parameters ( $A_\omega$ , in the first instance), the functional relation (26) turns out to be weak, so that  $\rho(A_\omega, r; [\phi])$  plays in this case the role of a sort of adiabatic invariant for 3-photon resonant ionization processes occurring under the action of the fields with slow-varying frequencies. Hence, an “almost-conservation” of  $\rho(A_\omega, r; [\phi])$  provides a simple and easily verifiable approximate criterion which enables the photoionization line profiles corresponding to different values/forms of the chirp to be compared and normalized.

The problem discussed here was first addressed, to our knowledge, in [32], within the framework of the similar 3-level model and for low pulse energies only. In contrast with our present approach, however, the genuine photoionization rate of the level  $|b\rangle$  (that is,  $2S$ ) was set in [32] equal, respectively, to zero and to some time- and energy-independent constant, while describing the dynamics of the 1st and the 2nd stages of the resonant 3-photon ionization. Although this approximation provides acceptable results for  $A_\omega \lesssim 6$  mJ, say, it is of interest, both experimental and theoretical, to reconsider the entire problem by releasing the above simplifying assumptions and getting, thereby, a deeper insight into the physics of the process.

**2.3.1. Low  $A_\omega$**  Let us consider first the simplest case of low  $A_\omega$ , such that condition (23) is satisfied. In addition, we will still assume, without a loss of generality, that the intensity of the incident radiation is Gaussian both in time and space, without specifying, though, particular form of the chirp for a moment. By making use of equation (16c), this allows  $\rho(A_\omega, r; [\phi])$  to be expressed in terms of  $\tilde{C}(x)$  as

$$\begin{aligned} \rho(A_\omega, r; [\phi]) &= \frac{c}{4\pi} \frac{2}{\omega_L} \sigma_b^{(\gamma)} \mathcal{I} \int_{-\infty}^{+\infty} d\Delta\nu \int_{-\infty}^{+\infty} dx \exp \left\{ -\frac{\tau^2 x^2}{2\sigma_t^2} \right\} \left| \tilde{C}(x, \Delta\nu, A_\omega, r) \right|^2 \\ &\times \exp \left\{ 2D_{b,a} \mathcal{I} \mathfrak{S} \left[ \int_{-\infty}^x \exp \left\{ -\frac{\tau^2 u^2}{2\sigma_t^2} \right\} \tilde{C}(u, \Delta\nu, A_\omega, r) du \right] \right\}. \end{aligned} \quad (27)$$

Here, our former notations (21) have been employed. To this end, it must be noted that  $|4\pi\tau\Delta\nu + 2\dot{\phi}(0) + \mathcal{I}\Delta D| \geq 1$  is satisfied for all  $\Delta\nu$  and  $\mathcal{I}$ , except those  $\Delta\nu$  which are in the vicinity of the lineshape's maximum,  $\Delta\nu \simeq -\dot{\phi}(0)/(4\pi\tau)$ , and for  $A_\omega$  such that  $|\mathcal{I}\Delta D| \lesssim 1$ . The latter condition happens to be more restrictive as compared to the one assumed here. This is due the fact that the diagonal matrix elements are usually much bigger than the non-diagonal ones (see table 1 for comparison). By making use of (25), (5) and presuming that the above condition is fulfilled, one can show that

$$2D_{b,a}\mathcal{I}\Im \left[ \int_{-\infty}^x \exp \left\{ -\frac{\tau^2 u^2}{2\sigma_t^2} \right\} \tilde{C}(u, \Delta\nu, A_\omega, r) du \right] \approx -\sqrt{2\pi}D_{b,a}^2 \mathcal{I}^3 \frac{\Im(\Delta D)}{\tau \left[ 4\pi\tau\Delta\nu + 2\dot{\phi}(0) + \mathcal{I}\Re(\Delta D) \right]^2 + \mathcal{I}^2[\Im(\Delta D)]^2} \left[ 1 + \operatorname{erf} \left( \frac{\tau x}{\sqrt{2}\sigma_t} \right) \right]. \quad (28)$$

Note that, for any  $x$ , arbitrary laser parameters and  $D_{b,a}$ , this expression is negative, as it should be, since  $\Im(\Delta D) = -\Im(D_{b,b}) = (4\pi\alpha)^{-1}\sigma_b^{(\gamma)}(\omega_L) > 0$ . For small pulse energies considered here, the right-hand side of (28) is proportional to  $\mathcal{I}^3$ , which permits the appropriate exponent in (27) to be expanded in terms of  $A_\omega$ . On retaining two leading terms in this expansion, this yields

$$\rho(A_\omega, r; [\phi]) = \frac{c}{4\pi} \frac{2}{\omega_L} \sigma_b^{(\gamma)}(\omega_L) \mathcal{I} \int_{-\infty}^{+\infty} d\Delta\nu \int_{-\infty}^{+\infty} dx \exp \left\{ -\frac{\tau^2 x^2}{2\sigma_t^2} \right\} \left| \tilde{C}(x, \Delta\nu, A_\omega, r) \right|^2 \times \left\{ 1 - \frac{\sigma_t}{\tau} \frac{\sqrt{2\pi}D_{b,a}^2 \mathcal{I}^3 \Im(\Delta D)}{\left[ 4\pi\tau\Delta\nu + 2\dot{\phi}(0) + \mathcal{I}\Re(\Delta D) \right]^2 + \mathcal{I}^2[\Im(\Delta D)]^2} \left[ 1 + \operatorname{erf} \left( \frac{\tau x}{\sqrt{2}\sigma_t} \right) \right] \right\}. \quad (29)$$

Further calculations are straightforward but cumbersome. Hence, some technical details will be given below for the first term in the curly brackets in (29) only; the corresponding contribution is denoted as  $\rho^{(0)}(A_\omega, r; [\phi])$ . In this simplest case, by substituting (25) for  $\tilde{C}(x)$  and interchanging the order of integration, one arrives at

$$\begin{aligned} \rho^{(0)}(A_\omega, r; [\phi]) &= \frac{c}{4\pi} \frac{\sigma_b^{(\gamma)}(\omega_L) \mathcal{I}^3}{\tau \omega_L} D_{b,a}^2 \int_{-\infty}^{+\infty} \exp \left\{ -\frac{\tau^2 x^2}{2\sigma_t^2} - \sqrt{2\pi} \frac{\sigma_t}{\tau} \mathcal{I} \Im(\Delta D) \operatorname{erf} \left( \frac{\tau x}{\sqrt{2}\sigma_t} \right) \right\} dx \\ &\quad \times \int_{-\infty}^x \exp \left\{ -\frac{\tau^2 u^2}{2\sigma_t^2} + \sqrt{2\pi} \frac{\sigma_t}{\tau} \mathcal{I} \Im(\Delta D) \operatorname{erf} \left( \frac{\tau u}{\sqrt{2}\sigma_t} \right) \right\} du \\ &= \frac{c}{4\pi} \frac{\sigma_t \sigma_b^{(\gamma)} \mathcal{I}^2}{\sqrt{2}\tau^2 \omega_L} \frac{D_{b,a}^2}{\Im(\Delta D)} \left\{ \sqrt{\frac{\pi}{2}} - \int_{-\infty}^{+\infty} \exp \left[ -2u^2 - \sqrt{2\pi} \frac{\sigma_t}{\tau} \mathcal{I} \Im(\Delta D) \operatorname{erfc}(u) \right] du \right\}. \quad (30) \end{aligned}$$

For two most important cases of interest,  $|\mathcal{I}\Im(\Delta D)| \ll 1$  and  $|\mathcal{I}\Im(\Delta D)| \gtrsim 1$ , the integral in (30) can be evaluated, respectively, by expanding the integrand into the power series in  $\mathcal{I}\Im(\Delta D)$  and by using the method of the steepest descent. This yields

$$\begin{aligned} &\int_{-\infty}^{+\infty} \exp \left[ -2u^2 - \sqrt{2\pi} \frac{\sigma_t}{\tau} \mathcal{I} \Im(\Delta D) \operatorname{erfc}(u) \right] du \\ &\quad \asymp \begin{cases} \sqrt{\pi/2} - \pi(\sigma_t/\tau) \Im(\Delta D) \mathcal{I} & \text{for } |\mathcal{I}\Im(\Delta D)| \ll 1 \\ (\sqrt{\pi}\tau^2/2^{3/2}\sigma_t^2) [\Im(\Delta D) \mathcal{I}]^{-2} & \text{for } |\mathcal{I}\Im(\Delta D)| \gtrsim 1 \end{cases}. \quad (31) \end{aligned}$$

Accordingly, we are left finally with

$$\begin{aligned} & \rho^{(0)}(A_\omega, r; [\phi]) \\ = & \frac{c}{4\pi} \sqrt{\frac{\pi}{2}} \frac{\sigma_t}{\tau^2 \omega_L} \sigma_b^{(\gamma)}(\omega_L) D_{b,a}^2 \times \begin{cases} \sqrt{\pi}(\sigma_t/\tau) \mathcal{I}^3 & \text{for } |\mathcal{I}\Im(\Delta D)| \ll 1 \\ [\sqrt{2}\Im(\Delta D)]^{-1} \mathcal{I}^2 & \text{for } |\mathcal{I}\Im(\Delta D)| \gg 1 \end{cases}. \end{aligned} \quad (32)$$

Note that in either limiting case, the result is independent, in accord with our initial statement, of particular form of the chirp  $\phi$ . To clarify this point, one should emphasize that the only two simplifications made in the course of derivation were: (i) the use of  $\tilde{C}(x)$  given by (25) and (ii) the replacement of the appropriate exponent by a unity. Both approximations are fully justifiable for  $A_\omega : |A_\omega D_{b,a}(\omega_L)| \lesssim 1$  assumed here. Obviously, the latter condition is consistent with the *first* relation in (32), which has been formerly obtained by means of a different technique (and cast in a slightly different analytic form) in [32]. Apart from being chirp-independent, this result demonstrates also that  $\rho^{(0)}(A_\omega, r; [\phi]) \propto A_\omega^3$ , as opposed to the next limiting case, that is,  $|\mathcal{I}\Im(\Delta D)| \gtrsim 1$ , where  $\rho^{(0)}(A_\omega, r; [\phi]) \propto A_\omega^2$ . A gradual decrease of the exponent is clearly evidenced by numerical simulations carried out by us for muonium, while scanning sufficiently broad  $A_\omega$ -domain. Some results of this numerical study are discussed in more detail in section 3 (see figure 8, for example). These show, in particular, that equations (32) describe  $\rho^{(0)}(A_\omega, r; [\phi])$  qualitatively correctly for both low and moderately high pulse energies.

In a similar manner one can also obtain appropriate contribution, denoted  $\rho^{(1)}(A_\omega, r; [\phi])$ , coming from the second term in the curly brackets in (29). After tedious calculations whose details will be given elsewhere, one ends up with the following expression for a sum of two contributions:

$$\begin{aligned} & \rho^{(0)}(A_\omega, r; [\phi]) + \rho^{(1)}(A_\omega, r; [\phi]) \\ = & \begin{cases} \frac{c}{4\pi} \frac{\pi}{\sqrt{2}} \frac{\sigma_t^2}{\tau^3 \omega_L} \sigma_b^{(\gamma)}(\omega_L) D_{b,a}^2 \mathcal{I}^3 \left(1 - \sqrt{2}\pi \frac{\sigma_t^2}{\tau^2} D_{b,a}^2 \mathcal{I}^2\right) & \text{for } |\mathcal{I}\Im(\Delta D)| \ll 1 \\ \frac{c}{4\pi} \frac{\sqrt{\pi}}{2} \frac{\sigma_t}{\tau^2 \omega_L} \sigma_b^{(\gamma)}(\omega_L) \frac{D_{b,a}^2}{\Im(\Delta D)} \mathcal{I}^2 \left(1 - \frac{4\sqrt{2}\pi}{3} \frac{\sigma_t^3}{\tau^3} D_{b,a}^2 \mathcal{I}^2\right) & \text{for } |\mathcal{I}\Im(\Delta D)| \gtrsim 1 \end{cases}. \end{aligned} \quad (33)$$

Here, according to (5), we have discarded the terms in  $\rho^{(1)}(A_\omega, r; [\phi])$  containing the second and higher order derivatives of  $\phi(x)$ . This simplification results in the fact that entire equation (33) turns out to be completely independent of the chirp.

The right-hand side of equation (5) depends (through  $\mathcal{I}$ ) on the radius  $r$ . To eliminate this dependence and to facilitate, thereby, an adequate comparison with the results of numerical calculations, the left- and right-hand sides of (5) can be integrated over the entire  $XOY$ -plane perpendicular to the direction of the laser beam's propagation ( $z$ -axis). A clear physical meaning of such an averaging procedure is discussed in the comments following equation (36).

By virtue of the identity,

$$\int_{-\infty}^{+\infty} \int_{-\infty}^{+\infty} \mathcal{I}^n dx dy = \frac{2\pi\sigma_r^2}{n} \left(\frac{2}{\pi c^2}\right)^{n/2} \left(\frac{\tau A_\omega}{\sigma_t \sigma_r^2}\right)^n \equiv \frac{2\pi\sigma_r^2}{n} \tilde{\mathcal{I}}^n, \quad n = 1, 2, \dots,$$

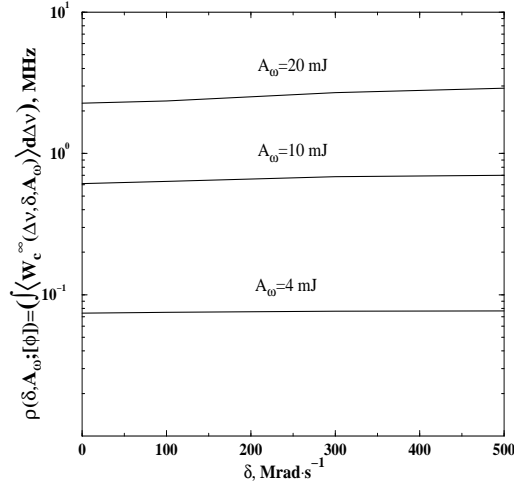


**Figure 4.** The integral of the spatially-averaged two-step 3-photon ionization probabilities of the ground state of muonium,  $\langle W_c^\infty(\Delta\nu, \delta, A_\omega) \rangle$ , over the entire range of the frequency detunings  $\Delta\nu$ , as a function of the chirp's magnitude,  $\delta$ ; three particular pulse energies are considered:  $A_\omega = 4, 10, 20$  mJ. The chirped frequency of the laser field employed is of the form:  $\nu(t) \equiv \nu_L + \nu_{\text{chirp}}(t) \equiv \nu_L + \frac{\delta}{4\pi} (1 + \text{erf}(t/\tau))$ . The rest laser parameters used are:  $\sigma_t = 51$  ns,  $\tau = 120$  ns,  $\sigma_r = 0.64$  mm.

which defines the spatially-independent part of  $\mathcal{I}$ , denoted as  $\tilde{\mathcal{I}} \equiv \sqrt{2/\pi c^2 \tau} A_\omega / \sigma_t \sigma_r^2$ , this yields eventually the following  $r$ -independent result:

$$\rho(A_\omega; [\phi]) \approx \int_{-\infty}^{+\infty} \int_{-\infty}^{+\infty} (\rho^{(0)}(A_\omega, r; [\phi]) + \rho^{(1)}(A_\omega, r; [\phi])) dx dy$$

$$= \begin{cases} \frac{c}{4\pi} \frac{\sqrt{2}\pi^2}{3} \frac{\sigma_t^2 \sigma_r^2}{\tau^3 \omega_L} \sigma_b^{(\gamma)}(\omega_L) D_{b,a}^2 \tilde{\mathcal{I}}^3 \left(1 - \frac{3\sqrt{2}\pi}{5} \frac{\sigma_t^2}{\tau^2} D_{b,a}^2 \tilde{\mathcal{I}}^2\right) & \text{for } |\tilde{\mathcal{I}}\Im(\Delta D)| \ll 1 \\ \frac{c}{4\pi} \frac{\pi^{3/2}}{2} \frac{\sigma_t \sigma_r^2}{\tau^2 \omega_L} \sigma_b^{(\gamma)}(\omega_L) \frac{D_{b,a}^2}{\Im(\Delta D)} \tilde{\mathcal{I}}^2 \left(1 - \frac{2\sqrt{2}\pi}{3} \frac{\sigma_t^3}{\tau^3} D_{b,a}^2 \tilde{\mathcal{I}}^2\right) & \text{for } |\tilde{\mathcal{I}}\Im(\Delta D)| \gtrsim 1 \end{cases} \quad (34)$$

In order to check this equation, the numerical calculation of  $\rho(A_\omega; [\phi])$ , in a wide range of  $A_\omega$  and for typical values of the rest physical parameters used in the 1S–2S experiment in muonium, have been carried out. This was done by an extra numerical integration of the 3-photon ionization line profiles  $\langle W_c^\infty(\Delta\nu, \delta, A_\omega) \rangle$  (see equation (36) for definition) over the entire  $\Delta\nu$ -domain. These results are shown in figure 4, for three particular pulse energies. At  $A_\omega = 4$  mJ, being the only value displayed which satisfies condition (23), the plot demonstrates that  $\rho(A_\omega; [\phi])$  is conserved to the 1% accuracy, within a wide range of the chirp's magnitude. The mean numerical value,  $\rho(A_\omega = 4 \text{ mJ}, \sigma_r = 0.64 \text{ mm}; [\phi]) \approx 0.080$  MHz, is to be compared with that obtained by means of the *first* equation in (34):  $\rho(A_\omega = 4 \text{ mJ}, \sigma_r = 0.64 \text{ mm}; [\phi]) \approx 0.1242 - 0.0292 = 0.095$  MHz. To make these results comparable, the latter value includes also an additional weighting factor,  $(9\pi\sigma_r^2)^{-1}$ . Even though parameter  $\lambda$  is very close to unity:  $\lambda = |\tilde{\mathcal{I}}\Im(D_{2s,2s})| \simeq |\tilde{\mathcal{I}}D_{2s,1s}| \approx 1$ , for  $A_\omega = 4$  mJ and  $\sigma_r = 0.64$  mm used here, numerical and analytical data are consistent to 20% of relative accuracy.

Interesting to note that the first/second relation in (34) overestimates/underestimate the true value of  $\rho(A_\omega; [\phi])$ . Much better agreement can be anticipated (and actually takes place) for lower pulse energies and/or bigger spatial dispersions  $\sigma_r$ . For  $A_\omega = 2 \text{ mJ}$  and  $\sigma_r = 1.5 \text{ mm}$  (appropriate line profiles are displayed in figure 5(a)), for example, numerical and analytical results read:  $\rho(A_\omega = 2 \text{ mJ}, \sigma_r = 1.5 \text{ mm}; [\phi]) \approx 0.90 \cdot 10^{-4} \text{ MHz}$  and  $(0.936 - 0.02) \cdot 10^{-4} = 0.916 \cdot 10^{-4} \text{ MHz}$ , respectively.

*2.3.2. High  $A_\omega$*  For higher pulse energies and/or smaller spatial dispersions  $\sigma_r$ , such that  $|\widetilde{\mathcal{I}\mathcal{S}}(\Delta D)| \gg 1$ , equation (34) fails to describe adequately the true function  $\rho(A_\omega; [\phi])$ . This refers both to the absolute values of  $\rho(A_\omega; [\phi])$  and, particularly, to its dependence on the magnitude of the chirp, which makes its appearance at high pulse energies. It has been elucidated above that the main underlying reason for this failure originates from the fact that “the linear approximation” ceases to be valid any longer, due to corrections caused by the  $C^2$ -term in equation (20). This non-linear term does not allow any reasonably accurate analytic treatment to be developed, so that the numerical analysis of the problem must be used instead. To simulate the high-energy regime, the results of our calculation are presented in figure 4, for two pulse energies,  $A_\omega = 10, 20 \text{ mJ}$ , and for typical values of the rest physical parameters used in the 1S–2S experiment in muonium. As in the case of low  $A_\omega$ , this was done by the numerical integration of the 3-photon ionization line profiles  $\langle W_c^\infty(\Delta\nu, \delta, A_\omega) \rangle$  over the entire  $\Delta\nu$ -domain. The plots demonstrate in fact a noticeable deviation of  $\rho(A_\omega; [\phi])$  from a constant value, with an increase of the pulse energy. For example, at  $A_\omega = 20 \text{ mJ}$  and for  $\delta$  in the range  $\delta = 0 \dots 500/(2\pi) \text{ MHz}$ , this deviation (that is, the dependence on the chirp’s magnitude) amounts already to 30%; in absolute units, the data read:  $\rho(A_\omega = 20 \text{ mJ}, \sigma_r = 0.64 \text{ mm}; [\phi]) = 2.265 \text{ MHz}$  for  $\delta = 0 \text{ MHz}$  and  $\rho(A_\omega = 20 \text{ mJ}, \sigma_r = 0.64 \text{ mm}; [\phi]) = 2.90 \text{ MHz}$  for  $\delta = 500/(2\pi) \text{ MHz}$ . Furthermore, the gauge of the given deviation may be expected to be even more pronounced at higher pulse energies, thus preventing us actually from viewing  $\rho(A_\omega; [\phi])$  as a conserving quantity in this case. Although such  $A_\omega$  are of no practical interest at the moment for the 1S–2S experimental study with muonium, the entire effect might be of relevance for future experimental studies where much higher laser intensities are involved.

### 3. Application to the experiment in muonium

Let us apply the results obtained in preceding sections to particular laser parameters adopted in the 1S–2S experiment in muonium [8], by assuming that  $|a\rangle \equiv 1S$ ,  $|b\rangle \equiv 2S$  and setting  $\phi(t) \equiv \delta t (1 + \text{erf}(t/\tau)) / 2$ . It is convenient in this section to measure the energies in the units:  $\hbar = e^2 = m^* = 1$ , where  $m^* = m_e / (1 + m_e/m_\mu) \approx (1.00484)^{-1} m_e$  stands for the reduced mass of the electron and muon. Here, the value for the electron to  $\mu^-$  mass ratio,  $m_\mu/m_e = 206.768262$ , was used. The quantity  $a^* \equiv \hbar^2 / (m^* e^2) = (m_e/m^*) a_0$  stands for the unity of distance, with  $a_0 = \hbar^2 / (m_e e^2) = 0.529 \cdot 10^{-8} \text{ cm}$  being the Bohr radius. Accordingly, one-particle energies and dynamic polarizabilities,

**Table 1.** The values of the two-photon matrix elements  $D_{b,a}$ ,  $(b,a) = 1s, 2s$ , defined by the sums in equations (10)-(12), and the value of the 1-photon photoionization cross section of the  $2S$ -level, given by (35), at  $\omega_L \approx 3/16$  a.u. ( $\lambda_L = 244$  nm); linear polarization of the photon,  $\epsilon$ , is assumed in both cases.

$D_{1s,1s}(\omega_L)$	$D_{2s,2s}(\omega_L)$	$D_{2s,1s}(\omega_L)$	$\sigma_{2s}^{(\gamma)}(\omega_L)$
-5.7141	29.8535 - i 12.8232	7.8535	0.2205

$\alpha_{b,a}^{ij}(\omega)$ , are measured in the units of  $e^2/a^*$  and  $(a^*)^3$ .

As was mentioned above, 3-photon ionization probability,  $W_c^\infty(\Delta\nu, \delta, A_\omega, r)$ , can be obtained by accurate numerically solving either the system (16b)-(16c) or (18a)-(18e). In both cases this has been done by the stepwise time integration, starting from  $t_0 = -3\sigma_t$ , while scanning sufficiently broad  $\Delta\nu$ -domain centered at  $\Delta\nu = 0$  (i.e.  $\omega_L = \frac{1}{2}\omega_{2s,1s}$ ), for all  $r \equiv \sqrt{x^2 + y^2}$  on the  $r$ -mesh:  $r_k = k\sigma_r/10$ ,  $k = 0 \dots 50$ . Numerical values of the matrix elements,  $D_{b,a}$ ,  $(a, b) = 1s, 2s$ , which enter (16b)-(16c) were calculated in [30, 17, 31]; these are compiled in table 1, together with the value of the single photoionization cross section of the  $2S$ -level at  $\omega = \omega_L$ . The latter is given explicitly by (see [31] and references therein)

$$\sigma_{2s}^{(\gamma)}(\omega_L) = \frac{2^{14}\pi^2}{3}\alpha \left(1 + 3\frac{I_{2s}}{\omega_L}\right) \left(\frac{I_{2s}}{\omega_L}\right)^4 \frac{e^{-4\eta \arctan(2/\eta)}}{1 - e^{-2\pi\eta}}, \quad \eta = \sqrt{\frac{4I_{2s}}{\omega_L - I_{2s}}} \quad (35)$$

where  $\alpha$  is the fine structure constant and  $I_{2s} = 1/8$  denotes the ionization potential of the  $2S$ -state.

At the final stage of our numerical procedure, a spatial averaging has been performed in order to obtain  $r$ -independent ionization profiles,  $\langle W_c^\infty(\Delta\nu, \delta, A_\omega) \rangle$ . This has been achieved by an extra integration of  $W_c^\infty(\Delta\nu, \delta, A_\omega, r)$  over entire  $XOY$ -plane perpendicular to the direction of the laser beam's propagation:

$$\langle W_c^\infty(\Delta\nu, \delta, A_\omega) \rangle \equiv \frac{1}{9\pi\sigma_r^2} \int_{-\infty}^{+\infty} \int_{-\infty}^{+\infty} W_c^\infty(\Delta\nu, \delta, A_\omega, r) dx dy. \quad (36)$$

Basically, this newly introduced quantity can be interpreted as an averaged ionization probability related to the entire laser beam spot, since  $\langle W_c^\infty(\Delta\nu, \delta, A_\omega) \rangle$  is independent of the distance from the beam's axis. Alternatively, in view of the low values of the muon density in the media [8] (see below),  $\langle W_c^\infty(\Delta\nu, \delta, A_\omega) \rangle$  can be called as "the ionization probability per one (muon) atom in the beam".

An auxiliary factor,  $1/(9\pi\sigma_r^2)$ , has been introduced in (36) in order to make  $\langle W_c^\infty(\Delta\nu, \delta, A_\omega) \rangle$  dimensionless, as the original probability  $W_c^\infty(\Delta\nu, \delta, A_\omega, r)$  is. This particular choice was adopted according to the so-called "3 $\sigma$ "-rule being inherent to various problems involving Gaussian law. In the case considered, the "3 $\sigma$ "-rule makes its appearance through the fact that the values of  $W_c^\infty(\Delta\nu, \delta, A_\omega, r)$  happen to be almost negligible for  $r > 3\sigma_r$ , unless the pulse energies higher than  $A_\omega = 20$  mJ, say, are considered. For such a high energy regime, the probability  $W_c^\infty(\Delta\nu, \delta, A_\omega, r)$  has a long-distance "tail" spreading out beyond the *effective* beam radius,  $r = 3\sigma_r$ , within which

the values of  $W_c^\infty(\Delta\nu, \delta, A_\omega, r)$  may be very close to, yet less than, 1. In this situation the proper normalization factor different from that chosen above must be used so as to prevent  $\langle W_c^\infty(\Delta\nu, \delta, A_\omega) \rangle$  from being bigger than 1. As is clearly evidenced by our calculations, the values of  $\langle W_c^\infty(\Delta\nu, \delta, A_\omega) \rangle$  defined by equation (36) exceed 1 starting already from  $A_\omega \simeq 20 \div 25$  mJ, depending on the rest laser parameters. One should point out, however, that such  $A_\omega$  are hardly attainable currently with proper pulsed lasers sources in the required frequency range. This makes the high energy regime in the resonant 3-photon ionization with muonium to be mostly of academic rather than practical interest at the moment, thus justifying the definition of equation (36). To avoid any misunderstanding, it must be clearly stated once again that the spurious effect mentioned here originates solely from the particular choice of the normalization factor in (36), and has, therefore, nothing to do with either the model developed in the work or a lack of the numerical accuracy employed by us. The latter was chosen to be equal to  $10^{-7}$  which proves to be sufficient to ensure that  $W_c^\infty(\Delta\nu, \delta, A_\omega, r) \leq 1$  holds (as it should!) for any particular individual set of all parameters involved in the problem, including  $r$ ,  $\Delta\nu$ ,  $\delta$ ,  $\tau$ , and  $\sigma_r$ .

The averaged probability  $\langle W_c^\infty(\Delta\nu, \delta, A_\omega) \rangle$  readily enables one to estimate the expected number of experimentally observed ionization events,  $N_{\text{event}}$ , defined as the number of the muonium atoms which are ionized by a sequence of  $N_{\text{shot}}$  identical Gaussian laser pulses (3) within the time  $T$  and detected eventually in apparatus. Such a formulation of the problem corresponds direct to the actual experimental situation where the gas media containing muonium atoms interacts with  $N_{\text{shot}} = 25$  laser pulses per second. Under these conditions, the required number of the ionization events to be detected during the observation time  $T \gg N_{\text{shot}}\tau$  can be estimated by means of the following simple relation:

$$N_{\text{event}} = \rho_0 \cdot S \cdot L \cdot T \cdot \eta \cdot N_{\text{shot}} \cdot W_c^{\text{max}}(\delta, A_\omega).$$

Here,  $\rho_0 \simeq 4 \cdot 10^{-3}$  atoms/mm<sup>3</sup> is the spatial density of the muonium atoms in the chamber,  $S = 9\pi\sigma_r^2 \simeq 11$  mm<sup>2</sup> and  $L \simeq 10^3$  mm stand, respectively, for the *effective* cross section of the laser beam (see above) and the total path which this beam travels in the media,  $\eta \simeq 10\%$  denotes an efficiency of registration of the muonium atoms in apparatus; finally,  $W_c^{\text{max}}(\delta, A_\omega)$  is the value of the averaged 3-photon ionization probability  $\langle W_c^\infty(\Delta\nu, \delta, A_\omega) \rangle$  at its maximum, for particular values of the chirp and the energy of the pulse. Provided  $\delta$  and  $A_\omega$  are fixed, this maximum is achieved approximately at  $\Delta\nu \approx -\delta/(4\pi)$ , almost independently of  $A_\omega$ , as can be seen in figure 5(b). In particular,  $W_c^{\text{max}}(\delta = 10 \text{ MHz}, A_\omega = 4 \text{ mJ}) \approx 0.014$  thus leading, for example, to the following expected number of events detectable during the observation time  $T = 3600$  s:  $N_{\text{event}} \simeq 5800$ . It is rather instructive that this value happens to be quite close to that found preliminary in the  $1S - 2S$  experiment in muonium being currently underway.

Some results of our simulations are presented in figures 5-9, for various magnitudes of the chirp  $\delta$  and various parameters of the laser pulse which are typically used in the

measurements of the  $1S - 2S$  energy separation in muonium; particular values employed are indicated in figures 5,6. Both these graphs demonstrate appreciable red-shift of the maxima (i.e. towards lower frequencies, relative to  $\nu_L = \omega_{2s,1s}/4\pi$ ) of the photoionization profiles with an increase of the chirp. It must be noted, however, that this shift is caused by a combination of two competing mechanisms: (i) the shift being due to the combined *AC Stark* effect for the  $1S$ - and  $2S$ -levels and (ii) that arising because of the chirp itself. The curves show that the former mechanism turns out to be small compared with the latter at relatively small pulse energies,  $A_\omega = 2 \dots 4$  mJ. At  $A_\omega = 4$  mJ and  $\delta = 0$ , for instance, i.e. in the case of completely unchirped laser signal, the *AC Stark* shift amounts approximately to 1 MHz. One can anticipate, however, that the relative contribution of the *AC Stark* shift will increase as the laser intensity increases, since its magnitude is linearly proportional to the laser intensity, whereas the chirp-induced shift is almost intensity-independent. This behaviour can be seen in figures 6(a,b) and is summarized in figure 7(a) showing, in particular, that the *AC Stark* shift becomes equals to 4 MHz at  $A = 20$  mJ,  $\delta = 0$ . In addition to the shift of the maxima, the curves in figures 5,6 exhibit a strong dependence on both the spatial dispersion  $\sigma_r$  and the power  $A_\omega$  of the laser signal. It should be noted that an appreciable distortion of the photoionization line shapes happens to be particularly enhanced at relatively large chirp values, where the line profiles become asymmetric. Generally speaking, this asymmetry is an intrinsic feature of the 3-photon resonant photoionization occurring under the action of the *chirped* pulsed laser signal. Moreover, an asymmetry of the

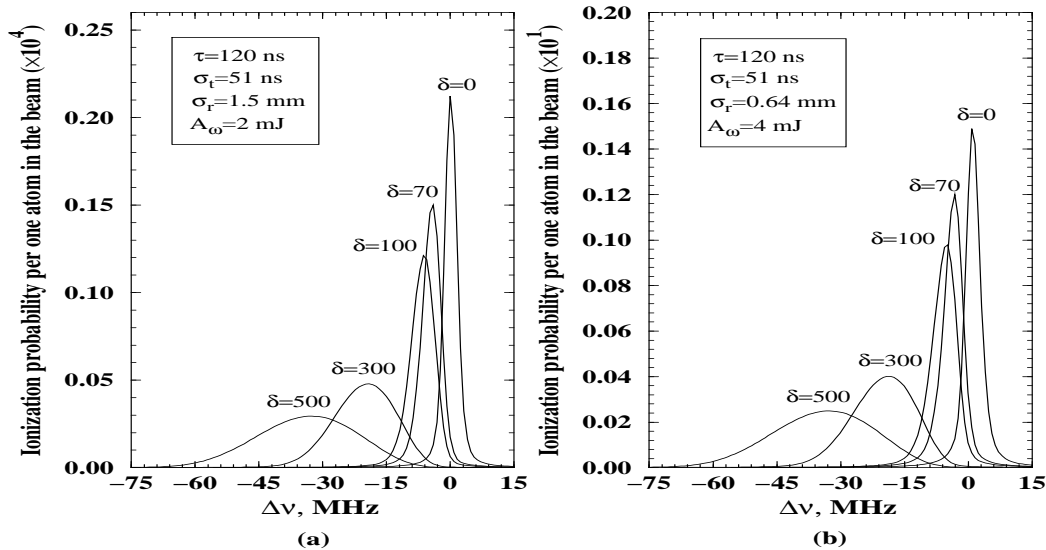


**Figure 5.** Two-step 3-photon ionization probabilities,  $\langle W_c^\infty(\Delta\nu, \delta, A_\omega) \rangle$ , of the ground state of muonium by the laser field with the chirped frequency  $\nu(t) \equiv \nu_L + \nu_{\text{chirp}}(t) \equiv \nu_L + \frac{\delta}{4\pi} (1 + \text{erf}(t/\tau))$ ,  $\delta = 500, 300, 100, 70, 0$  Mrad  $\cdot$  s $^{-1}$ , versus laser frequency detuning,  $\Delta\nu \equiv (\omega_L - \frac{1}{2}\omega_{2s,1s})/2\pi$ . Two pairs of different values for the pulse energy,  $A_\omega$ , and the spatial dispersion of the laser signal,  $\sigma_r$ , are used: (a)  $A = 2$  mJ,  $\sigma_r = 1.5$  mm, and (b)  $A = 4$  mJ,  $\sigma_r = 0.64$  mm.

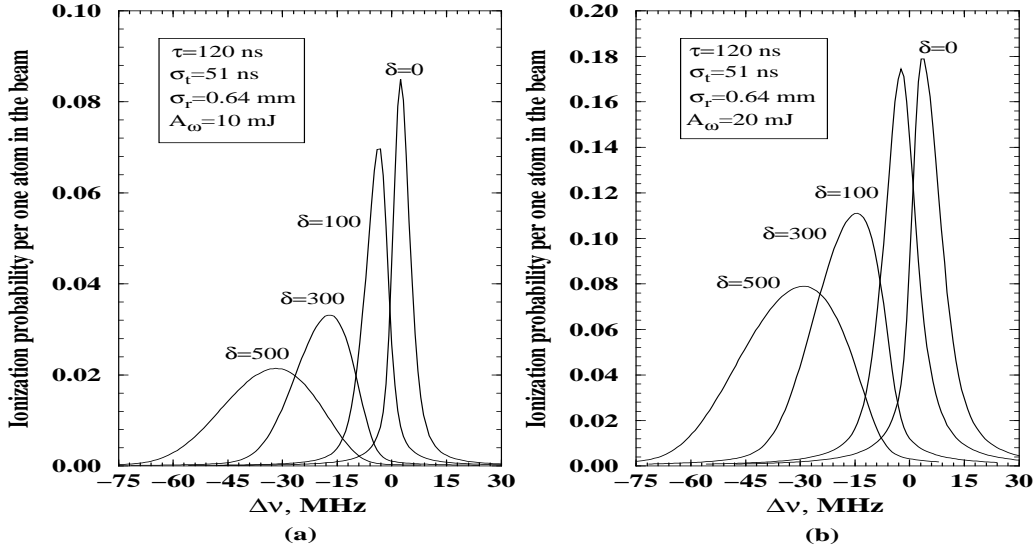


**Figure 6.** Two-step 3-photon ionization probabilities,  $\langle W_c^\infty(\Delta\nu, \delta, A_\omega) \rangle$ , of the ground state of muonium by the laser field with the chirped frequency  $\nu(t) \equiv \nu_L + \nu_{\text{chirp}}(t) \equiv \nu_L + \frac{\delta}{4\pi} (1 + \text{erf}(t/\tau))$ ,  $\delta = 0, 100, 300, 500 \text{ Mrad} \cdot \text{s}^{-1}$ , versus laser frequency detuning,  $\Delta\nu \equiv (\omega_L - \frac{1}{2}\omega_{2s,1s})/2\pi$ , for two pulse energies: (a)  $A_\omega = 10$  mJ and (b)  $A_\omega = 20$  mJ.

ionization line shapes happens to be one of the most pronounced manifestations of the non-monochromaticity of the laser field. This phenomenon is basically due to the fact that the chirp, even though its relative magnitude amounts to only  $\delta/\omega_L \simeq 10^{-8} \dots 10^{-7}$  in our calculations, violates an equivalence of initial ( $t = -\infty$ ) and final ( $t = +\infty$ ) time

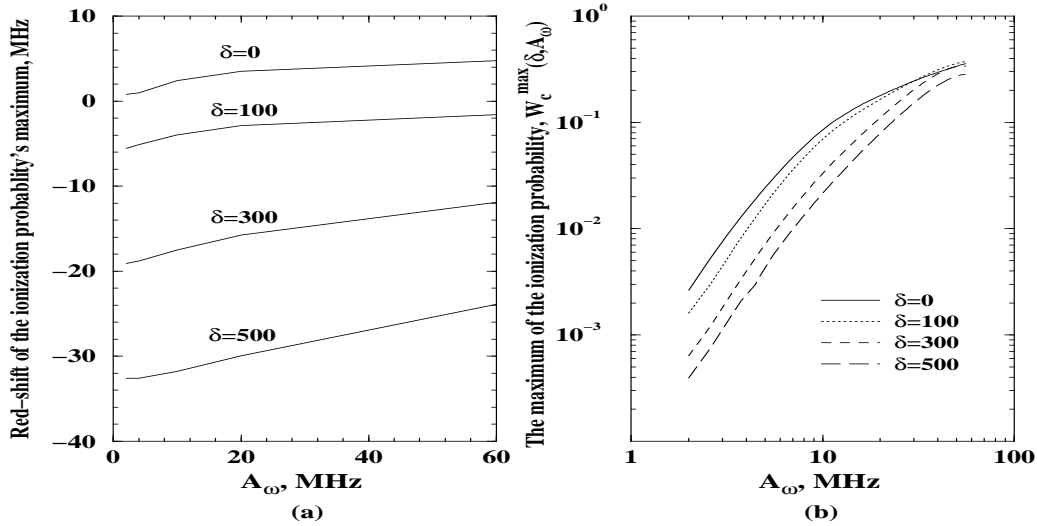


**Figure 7.** (a) - the frequency red-shift of the photoionization profile's maximum, against the pulse power  $A_\omega$ . The chirped frequency of the laser field is assumed to be of the form:  $\nu(t) \equiv \nu_L + \nu_{\text{chirp}}(t) \equiv \nu_L + \frac{\delta}{4\pi} (1 + \text{erf}(t/\tau))$ ,  $\delta = 0, 100, 300, 500 \text{ Mrad} \cdot \text{s}^{-1}$ ; (b) - the power-dependence of the line profile's maximum value. In both cases the rest laser parameters are the same as in figures 6(a,b).

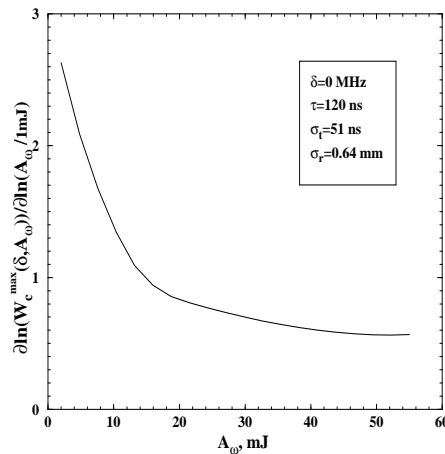


**Figure 8.** The  $A_\omega$ -dependence of the exponent,  $\mu(A_\omega)$ , defined by the relation:  $W_c^{\max}(\delta, A_\omega) = \gamma(\delta)A^{\mu(A_\omega)}$ .

moments. Indeed, the photoionization probability turns out to be either more efficient or suppressed, depending on whether the time-dependent chirped laser frequency is in the resonance with the 2-photon  $|a\rangle \rightarrow |b\rangle$  transition or slightly off it. The process as a whole becomes then somewhat “time-sensitive”, although the form of the laser pulse envelope used is time-invariant. It should be noted, however, that the gauge of the above asymmetry depends strongly on the laser power, as well as particular forms of the laser amplitude and the chirp. This dependence can be seen in figures 6(a,b) where higher  $A_\omega$ -values as compared with figures 5(a,b) are used. The former show that the asymmetry discussed is less pronounced as long as higher laser intensities are involved. Two essential characteristics of the line profiles’ maximum, that are, the shift and the magnitude, are plotted in figure 7(a,b) as functions of the laser power for various values of the chirp. In particular, the graph 7(b) provides information about the dependence of the line shapes’ maximum value,  $W_c^{\max}(\delta, A_\omega)$ , on the pulse energy  $A_\omega$ . It is quite natural to parameterize this relation by the following simple power law:  $W_c^{\max}(\delta, A_\omega) = \gamma(\delta)A^{\mu(A_\omega)}$ . The exponent here proves to be a slow-varying function of the pulse energy, such that  $(d\mu(A_\omega)/dA_\omega)/\mu(A_\omega) \ll (A_\omega \ln A_\omega)^{-1}$ . According to this condition,  $\mu(A_\omega)$  can be estimated as

$$\mu(A_\omega) \approx \frac{\partial}{\partial(\ln A_\omega)} \ln [W_c^{\max}(\delta, A_\omega)].$$

One should note, for example, an appreciable deviation of the  $\mu(A_\omega)$ -values from 3 which must be expected for a 2-step 3-photon ionization of an atom in the state  $|a\rangle$  by a *weak, monochromatic and spatially homogeneous laser field*, without the relaxation of the intermediate levels. For  $\delta = 0$ , the  $A_\omega$ -dependence of  $\mu(A_\omega)$  is displayed in figure 8. This graph demonstrates that  $\mu(A_\omega = 2 \text{ mJ}) \approx 2.75$  gradually decreases as the pulse energy increases and tends, for  $A_\omega \gg 20 \text{ mJ}$ , to an almost constant value,  $\mu \approx 0.5$ , thus

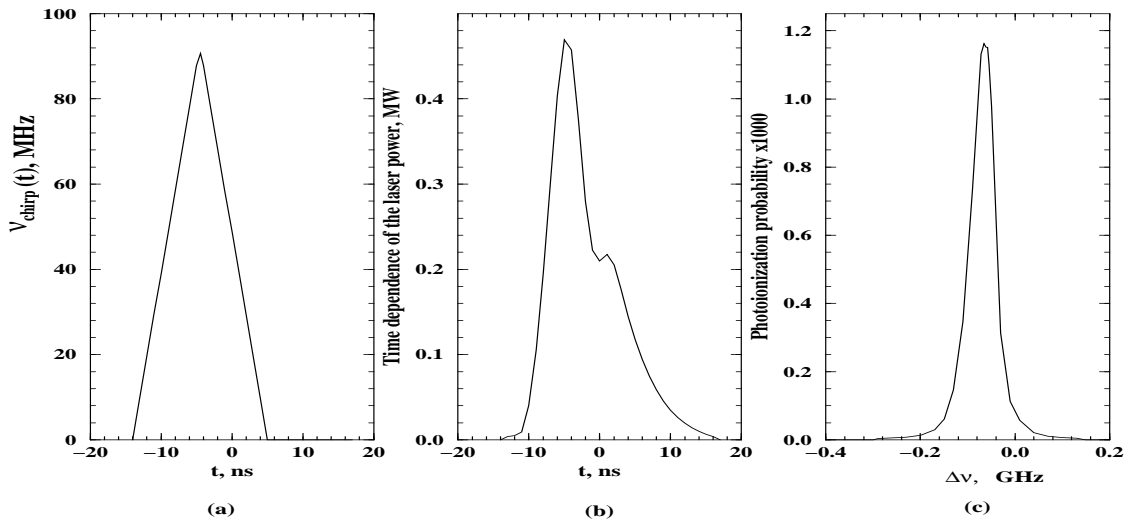


**Figure 9.** Time-dependence of the chirp – (a) – and the laser power – (b) – both detected in the former experimental measurements of the  $1S - 2S$  separation in muonium [8]; (c) - photoionization line profile measured in [8], versus laser frequency detuning,  $\Delta\nu \equiv (\omega_L - \frac{1}{2}\omega_{2s,1s})/2\pi$ .

indicating on the presence of saturation in the 3-photon transition considered.

Finally, it should be mentioned that the above consideration has been developed mainly in the attempt to simulate those line profiles of the two-step 3-photon ionization probabilities that are supposed to be measured soon in the new  $1S - 2S$  experimental investigation of muonium. Essential physical parameters employed in this study are still not fixed completely and are subject to further changes. It is therefore rather tempting to apply our present technique to appropriate data formerly collected within the framework of the previously employed experimental setup [8]. These are shown in figures 9(a,b), along with the photoionization line profile obtained within the framework of the current theoretical approach, figure 9(c). The fact that the corresponding experimental line shape (not shown) is virtually indistinguishable from the theoretical one provides an additional and independent check of the overall validity of the model developed in this work.

#### 4. Conclusion

We have developed a simple theoretical scheme intended to describe, to the 1 MHz accuracy, the stepwise 3-photon resonant photoionization in hydrogenic systems, induced by the chirped laser field with time-dependent amplitude. It has been shown that such an accuracy can be achieved within the framework of a simple 3-level model, by taking into account (i) the *AC Stark* shifts and (ii) non-zero ionization rates of the levels involved, together with (iii) a spatial inhomogeneity of the laser signal and (iv) arbitrary  $t$ -dependencies of its intensity (pulse envelope),  $I(\mathbf{r}, t)$ , and frequency,  $\omega(t)$ . The system of equations (16b)-(16c) or, equivalently, equations (18a)-(18e) is a key point

of the method employed. These are of independent significance as being not specifically restricted to particular states of reference, laser intensities, and chirps, so that the results obtained for  $1S-$ ,  $2S-$  and  $\varepsilon P-$  states can be generalized on arbitrary  $|a\rangle$ ,  $|b\rangle$ ,  $|c\rangle$  levels of hydrogen-like atoms. Excited  $ns-$  levels, such that  $2 \leq n \leq 5$ , are of particular current interest for ultra-high precision laser spectroscopy, and it should be expected that an adequate interpretation of experimental data should require an accurate theoretical account of a wide spectrum of light-induced effects. Some of these effects are beyond the scope of our present consideration and, in the first instance, comprise appropriate corrections due to inevitable motion of atoms in the media and associated *second* order Doppler shifts, as being of major importance. Indeed, even for CW lasers where the signals are usually almost unchirped in the laboratory frame, the amplitude and the frequency of the pulsed laser signals become essentially time-dependent in the atomic rest frame, thus leading, as was demonstrated above, to the shifts and distortions of ionization/excitation lines. The relative contribution of the effects discussed is estimated as  $\alpha^2 v_z^2$  with  $v_z$  being the atomic velocity in the laboratory frame, and these should be incorporated in the theoretical scheme developed here, along with relativistic/radiative corrections  $\simeq \alpha^2$  to the operator of the particle-laser field interaction. This work is currently in progress, and we consider it as a subject of forthcoming publications.

### Acknowledgments

The authors are indebted to G. zu Putlitz for his constant support and encouragement. This work has been strongly motivated and influenced by discussions within the muonium 1S-2S collaboration, particularly with P.E.G. Baird, M.G. Boshier, P.G.H. Sandars, and W.T. Toner. One of us (V.Y.), wishes to acknowledge his gratitude to Prof. I.P. Grant (FRS) for his kind advice and to the Volkswagen-Stiftung and the Royal Society for financial support. Also, this work has been funded in part by the grants from NATO, the Royal Society and the Bundesminister für Bildung und Forschung of Germany.

## References

- [1] Nez F, Plimmer M D and Bourzeix S 1993 *Europhys. Lett.* **24** 635
- [2] Bourzeix S *et al* 1996 *Phys. Rev. Lett.* **76** 384
- [3] Berkeland D, Boshier M D and Hinds E 1995 *Phys. Rev. Lett.* **75** 2470
- [4] Schmidt-Kaler F, Leibfried D, Seel S *et al* 1995 *Phys. Rev. A* **51** 2789
- [5] Udem Th, Huber A *et al* 1997 *Phys. Rev. Lett.* **79** 2646
- [6] Fee M S, Chu S, Mills A P *et al* 1993 *Phys. Rev. A* **48** 192
- [7] Mills Jr. A P 1993 *Hyperfine Interactions* **76** 233
- [8] Maas F E *et al* 1994 *Phys. Lett.* **A187** 247
- [9] Jungmann K 1995 *Physikalisches Blätter* **51** 1167
- [10] G. zu Putnitz 1996 *Hyperfine Interactions* **103** 103
- [11] Boshier M G, Hughes V W, Jungmann K and zu Putnitz G 1996 *Comments Atom. Mol. Phys.* **33** 17
- [12] Eikema K S, Ubachs U, Vassen W and Hogervorst W 1997 *Phys. Rev. A* **55** 1866;  
—1997 *Phys. Rev. Lett.* **71** 1690
- [13] Giacobino E and Cagnac B 1980 *In Progress in Optics XVII* ed E Wolf (Amsterdam: North-Holland) pp 86-161
- [14] Zon B A 1974 *Opt. Spectrosc.* **36** 838
- [15] Zon B A and Katsnel'son B G 1973 *Sov.Phys.-JETP* **65** 947
- [16] Zon B A, Manakov N L and Rapoport L P 1975 *Opt. Spectrosc.* **38** 6
- [17] Beausoleil G R and Hänsch T W 1986 *Phys. Rev. A* **33** 1661
- [18] Kaplan A E 1973 *Sov.Phys.-JETP* **65** 1416
- [19] Kaplan A E 1975 *Sov.Phys.-JETP* **68** 823
- [20] Lifshitz E M and Pitaevskii L P 1974 *Relativistic Quantum Theory. Course of Theoretical Physics, Part I, vol 4* (Oxford: Pergamon)
- [21] Landau L D and Lifshitz E M 1974 *Nonrelativistic Quantum Theory. Course of Theoretical Physics, vol 3* (Oxford: Pergamon)
- [22] Bakule P, Cornish P S, Lane I, Baird P E G, Toner W T, Sandars P G H, Liu W, Towrie M, *Private communication*
- [23] 1970 *Handbook of Mathematical Functions* ed M Abramowitz and I Stegun (Dover, New York).
- [24] Cohen-Tannoudji C 1968 *Cargese Lectures on Physics* vol 2 (Gordon and Breach: N.Y.)
- [25] Levinson M D 1982 *Introduction to Nonlinear Spectroscopy* (Academic: New York)
- [26] Salzman W R 1971 *Phys. Rev. Lett.* **26** 220
- [27] Vasilenko L S, Chebotaev V P and Shishaev A V 1970 *Pis'ma Zh. Eksp. Teor. Fiz.* **12** 161
- [28] Bloembergen N and Levensen M D 1976 *High Resolution Laser Spectroscopy* ed K Shimoda (Springer, Berlin) p 315
- [29] Sargent III M, Scully M O and Lamb Jr. W E 1974 *Laser Physics* (Reading, Mass.: Addison-Wesley)
- [30] Bassani F, Forney J J and Quattropani A 1977 *Phys. Rev. Lett.* **39** 1070
- [31] Yakhontov V and Jungmann K 1996 *Z. Phys. D* **38** 141
- [32] Woodman J 1992 *Ph.D. Thesis*, University of Oxford, Clarendon Laboratory (unpublished)